Available online at www.sciencedirect.com
ScienceDirect
Electric Power Systems Research 78 (2008) 559–565
ELECTRIC POWER SYSTEMS RESEARCH
www.elsevier.com/locate/epsr

Denoising using wavelets on electric drive applications☆

D. Giaouris, J.W. Finch*

School of Electrical, Electronic & Computer Engineering, Newcastle University, Newcastle upon Tyne NE1 7RU, UK

Received 17 March 2006; received in revised form 5 February 2007; accepted 4 May 2007
Available online 22 June 2007

Abstract

One common problem in drives applications is the presence of noise that corrupts the useful information in measurements such as of current, due to sensor imperfections. Digital low pass filters are a solution to the problem but they cannot cope when the useful information has time varying high frequency characteristics. In this paper, wavelet analysis, seldom used as yet in electric drives, is analysed and compared to classical methods. The key points of wavelet analysis are presented in a way that is appropriate for drives. Application of this new method to a typical practical current signal demonstrates the advantages and limitations of these methods over more conventional techniques. The true power of the wavelet transform is revealed when it is applied to a speed estimation problem where the rotor speed of a permanent magnet machine is modulated and coupled with high frequency components.

Keywords: Induction motor; Electric drives; Wavelet analysis; Current denoising; Multiresolution

1. Introduction

The wavelet transform (WT) has been extensively used in the digital image and signal processing areas in applications where the classical Fourier transform (FT) cannot cope. In refs. [1,2], two well known authors describe the WT from a digital image/signal processing point of view. A renowned paper on wavelets, by Daubechies [3], analyses frames and orthogonal wavelets in great depth. Mallat [4] sets the foundations for the fast WT (FWT), making the WT more attractive for online applications. For electric drives its application appears to have been relatively limited, for example, to off-line studies of the system's parameters [5,6]. In ref. [5], the modelling of the motor and especially the field distribution in the air gap is accomplished with the use of the simple Haar (or Daubechies 1—DB1) wavelet. On-line applications have been quite limited, but include fault diagnosis, neural network training and position signal de-noising [6–8].

The goal of this paper is hence to introduce the on-line application of the WT in the area of drives and to demonstrate its utility. A review of the theoretical aspects of the WT is first presented in a way suitable for drives applications, building on general reference material [9–12]. Test results from a wavelet denoising scheme are shown, from a real application using currents signals taken from an inverter fed induction machine (IM) drive. It is shown that when the useful information is closely defined in frequency, and well separated from the noise frequency components, then the WT and a more conventional digital filter gave similar results. The complexity of the WT can cause problems when used in real time applications, and in such a case would offer no advantage.

The WT can offer significant advantage in other cases. This is illustrated in the last part of this paper which studies the use of wavelets in a speed estimation scheme involving high frequency injection. Conventional methods have difficulty distinguishing between noise and the modulated rotor speed, while wavelets are successful in reducing the mean squared error.

2. Wavelets transform theory

2.1. Introduction

Action to reduce the noise on a signal is a common requirement in an electric drive scheme. A usual choice is a low pass filter, often a finite impulse response (FIR) filter, with its design based on the well-known concept of the FT. The kernel of this

☆ Dr. Giaouris and Professor Finch are with the Electrical Drives Group, School of Electrical, Electronic & Computer Engineering, Newcastle University, Newcastle upon Tyne NE1 7RU, UK.
* Corresponding author. Tel.: +44 191 222 7326; fax: +44 191 222 8180.
E-mail address: j.w.finch@ncl.ac.uk (J.W. Finch).

0378-7796/$ – see front matter © 2007 Elsevier B.V. All rights reserved.
doi:10.1016/j.epsr.2007.05.004

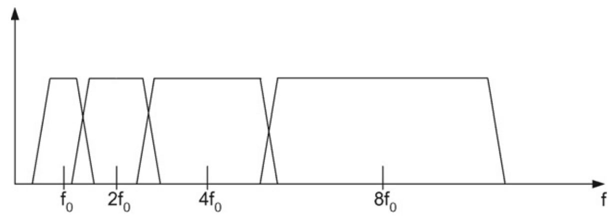

Fig. 1. Logarithmic coverage of the frequency spectrum under the WT.

transform is the exponential term $e^{-j\omega}$ (or $e^{j\omega}$ or $e^{-j2\pi f}$). This kernel extends from minus infinity to plus infinity in frequency and hence any non-stationary noisy signals cannot be isolated and removed. Therefore, any denoising method based on the FT will have the handicap of the priori assumption that the noisy signal is stationary. Finally, although of lesser significance, a small error in the time domain can cause a large distortion of the frequency spectrum even if only off-line study is required. One of the characteristics/properties of the WT is its ability to identify discontinuities. This has started to be used in the drives area since faults (in bearings, phase coils, etc.) can cause abrupt changes in the stator/rotor currents which wavelets can detect [13,14].

A first solution to these problems was the use of the short time FT (STFT), first proposed by Gabor almost 60 years ago. The signal is separated into several segments and then the FT is applied in every segment separately. Hence, the segment in which a high frequency component exists can at least be identified [15]. Unfortunately, the smaller the time window (for better time resolution) the worst the frequency resolution [1,2] (Heisenberg uncertainty theory). Hence, a trade off must be made between good time and frequency resolution.

2.2. Continuous and discrete time wavelet analysis

Fortunately the signals often found in practice have large duration low frequency, and small duration high frequency, components. Hence, it would be desirable to have small time windows for the high frequency parts and long windows for low frequencies. This can be achieved by imposing a restriction on the frequency window:

$$\frac{\Delta f}{f} = \text{constant.} \tag{1}$$

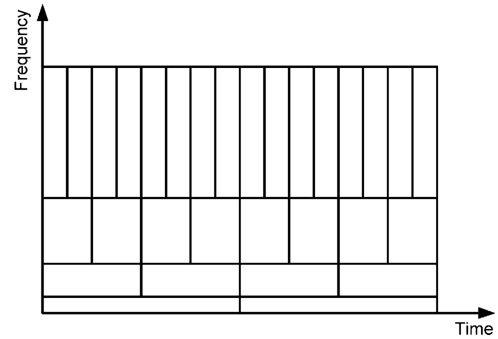

Fig. 2. Time frequency plane for the WT.

This results in a logarithmic coverage of the frequency spectrum (Fig. 1).

Again the uncertainty principle is satisfied but now the time resolution becomes arbitrarily good (small Δt) for high frequencies and vice versa, i.e. the frequency resolution becomes arbitrarily good (small Δf) for low frequencies (Fig. 2). This is the concept of multiresolution (Fig. 3).

The kernel is required not to be a sine or cosine wave but one signal well concentrated in time and in frequency—an asymmetric irregular waveform, i.e. a wavelet, such as that shown in Fig. 4, whose frequency spectrum is that of a band pass filter as proved later.

This wavelet can be scaled (contracted or dilated) and shifted. The transformation is accomplished in a similar way to the STFT, a portion of the signal is compared with the wavelet and their correlation is the coefficient for this scale and shift. Then the wavelet is shifted and compared with another segment of the signal. When all segments are compared the wavelet is compressed (or stretched) and the same comparison takes place. Therefore, the outcome coefficients are a function of the scale and shift:

$$C(a,b) = \int x(t)\overline{\psi(at+b)}\,\mathrm{d}t = |a|^{-1/2}\int x(t)\overline{\psi\left(\frac{t-b}{a}\right)}\,\mathrm{d}t \tag{2}$$

where "a" and "b" are the scaling and the shifting factors, respectively. The term $|a|^{-1/2}$ is only needed for energy normalisation. The function "ψ" is called the mother wavelet and a very large value of the scale means a global view of the signal. The inverse

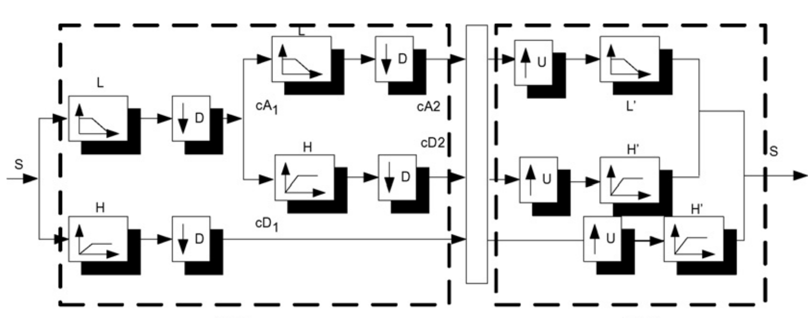

Fig. 3. Multiresolution wavelet analysis and synthesis.

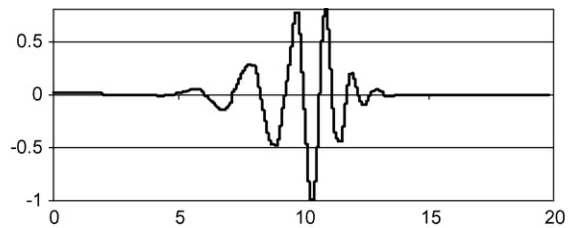

Fig. 4. DB10 wavelet.

WT (IWT) is given by the "resolution of identity":

$$x(t) = C_{\Psi}^{-1} \int_{-\infty}^{\infty} \int_{-\infty}^{\infty} \frac{1}{a^2} \langle x, \psi(a, b, t) \rangle \psi(a, b, t) \, \mathrm{d}a \, \mathrm{d}b \tag{3}$$

where

$$C_{\Psi} = 2\pi \int_{-\infty}^{\infty} (|\Psi(\omega)|^2 |\omega|^{-1}) \, \mathrm{d}\omega. \tag{4}$$

From Eqs. (3) and (4), it can be seen that $C_{\Psi}^{-1} > 0$ or $C_{\Psi} < \infty$. Hence, by using Eq. (4) it can be seen that the wavelet vanishes at zero frequency, i.e. $|\Psi(0)|^2 = 0$. This means that the wavelet is like a band pass filter and its average value, in the time domain, is zero: $\int \psi(t) \, \mathrm{d}t = 0$. This is the admissibility condition.

Eq. (2) implies there is an infinite number of scales and shifts that must be used for the WT, this can cause unnecessary redundancy in the transformation. The discrete time WT (DTWT) can be used to avoid this implication. The basic property of the DTWT is that every scale is represented by a dyadic filter and the wavelet coefficients for each shift are the output of two filters (one low pass and the other high pass). Hence, by using high and low pass (usually FIR) filters it is possible to implement online the DTWT.

2.3. Wavelet denoising

The high and the low frequency coefficients are termed details and approximations, respectively. Donoho [16] first proposed a method to denoise a signal by using the DTWT and a threshold. There are two main variations of this method: soft thresholding and hard thresholding [17,18]. These methods imply that by using an appropriate operator on the coefficients of the WT the signal can be denoised.

A measurement consists of the useful signal and the noise:

$$M(t) = x(t) + N(t) \tag{5}$$

By using Eq. (2) the wavelet coefficients can be found, C.

The denoising process is:

$$Z = D(C, q) \tag{6}$$

where q is a parameter that will be used later to denoise the signal.

The IWT of the denoised signal will give the estimated original signal $\tilde{x}$. (7)

When the method of soft thresholding is used the operator D is:

$$D(C, q) = \mathrm{sgn}(C) \times \max(0, |C| - q) \tag{8}$$

At the hard threshold the operator D is only nullifying the values of the wavelet coefficient that are less than the value of q:

$$D(C, q) = \begin{cases} C, & \text{if } |C| > q \\ 0, & \text{otherwise} \end{cases} \tag{9}$$

A similar method will be applied in this paper. As shown later the maximum level that the analysis will reach is 5. Furthermore in a typical drives application in the constant torque region the useful information is often at low frequency, perhaps between 0 and 50 or 60 Hz. Also the noise components will usually have much higher frequency. Hence, all the details coefficients will represent noise. So zeros can replace these coefficients and hence the reconstruction process will involve only approximations.

3. Wavelet filtering

3.1. Experiment arrangement

The practical signal used to test the filtering can be seen in Fig. 5. This was measured on a modern 4-pole 400 V, delta connected 7.5 kW induction motor based electrical drive coupled to a dc load machine, being driven by a commercial inverter. The particular waveform results from the drive undergoing a simple voltage proportional to frequency acceleration from 0 to 10 Hz in 0.2 s with no load. The current waveform from phase A of the motor drive is shown.

Initially the best level of decomposition and wavelet was found and then this was compared with the performance of a normal FIR filter. Five different levels of analysis were tested and the wavelets that were used are from the Daubechies family, DB2–DB43 (DB1 is the Haar wavelet and should not be used for multiresolution). The sampling frequency was chosen to be 10 kHz.

Since the test signal used is a practical signal already contaminated by noise, the ideal or noise-less signal is not available directly, as it would be if a simulation signal and noise sources were used. Since a more effective comparison can be made if a version of the ideal were available, the practical signal of Fig. 5 was filtered by an ideal analogue low pass sixth-order Butterworth filter with a cut off frequency of 60 Hz. Such a low cut-off

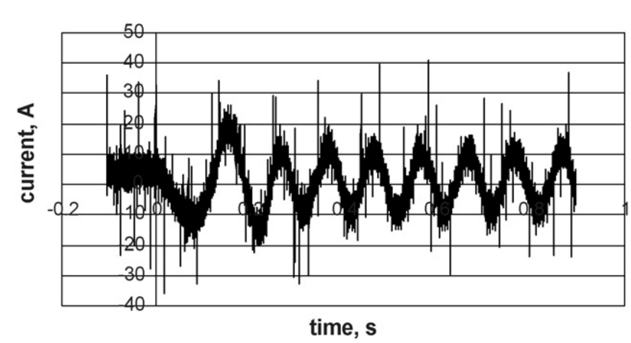

Fig. 5. Current i_{sA} that was used to check the wavelet denoising schemes.

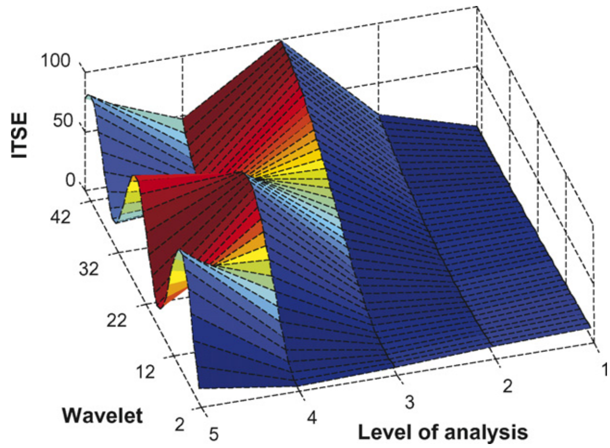

Fig. 6. ITSE for different wavelets and level of decomposition.

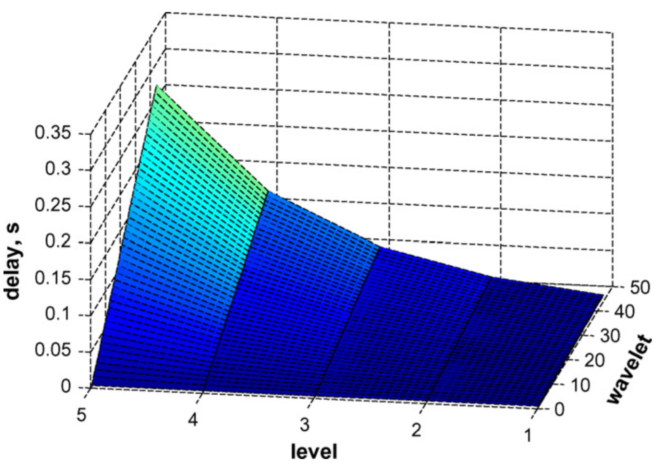

Fig. 7. Delay imposed by different wavelets and level of decomposition.

frequency would be impractical in an actual drive expected to run over a range of frequency.

This "ideal" de-noised signal was then compared with the response of the multiresolution and the Integral of Square Error (ITSE) was calculated (Fig. 6). Since simple FIR filters are used for the signal denoising in the WT scheme and since different sampling rates are used (due to the decimation) a certain delay is imposed which is equal to $(2^{\text{number of filters}} - 1)$ (also called the data alignment, which is very important for real time applications). This delay is the explanation for the peculiar form of Fig. 6. Normally it would be expected that the higher the decomposition number the better the denoising, but then the imposed delay will have a bigger effect. Fig. 7 shows the relation between the level of the decomposition, the wavelet and the delay. If the decomposition employs many levels then a significant delay will be imposed on the signal and, in an extreme case, this may even cause instability. Fig. 6 shows that level 4 gave considerably better results than level 2. Hence, a level 4 wavelet DB2 was chosen for comparison with a normal FIR filter. A low pass FIR filter was tested for this comparison. The specification of this filter is shown in Table 1.

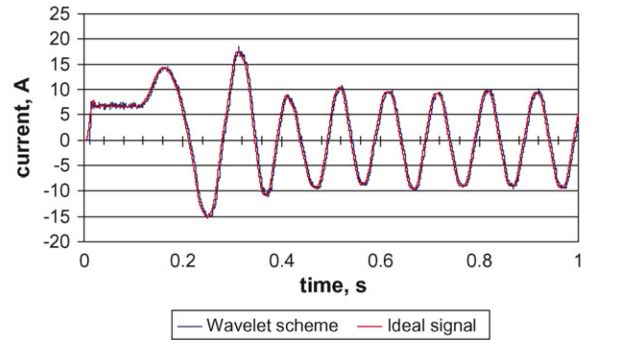

Fig. 8. Denoised stator signals, phase A, using an "ideal" and a wavelet filtering process.

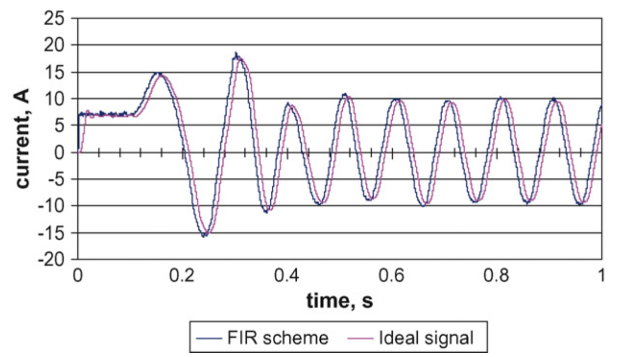

Fig. 9. Denoised stator signals, phase A, using an "ideal" and a FIR filter.

3.2. Tests results

3.2.1. Simple denoising

The ideal reference signal produced by the Butterworth filter and the version from the wavelet denoising scheme described above are shown in Fig. 8. The denoising of the FWT is almost identical to that of the analogue filter. The only significant difference is a small delay that is imposed on the FWT from the successive asymmetric FIR filters, clearly the analogue filter being of relatively high order does also introduce a significant delay, this causes the two signals to be closely similar.

The FIR scheme response is shown in Fig. 9, again with the "ideal" signal for comparison. The results of Figs. 8 and 9 show the wavelet denoising scheme gave similar results to the carefully chosen normal FIR filter on a fixed spectrum signal. Fig. 12 shows that the FIR scheme produced an output faster than the analogue filter. This is expected since the delay of that

Table 1
FIR filter used for comparison with wavelet denoising schemes

Filter	Passband frequency	Passband ripple	Stopband frequency	Stopband ripple	Sampling frequency	Filter order
FIR	100 Hz	0.624 dB	500 Hz	33.3 dB	10 kHz	40

digital filter is very small, i.e. is smaller than that of the analogue filter.

The last figures show that the two schemes have similar denoising behaviour, but the wavelet scheme imposes a delay (which will increase if more levels of decomposition are added to achieve better denoising). Also it is more complicated. The FIR scheme uses a simple symmetrical FIR filter which can be implemented either with simple and cheap hardware or with some addition to the overall drives software. The FWT scheme needs more complicated and asymmetric FIR filters, with a complexity increase of at least 10 times. Hence, the FIR scheme appears superior in such a case, and therefore for many simple denoising processes in electric drives it is better to use classical filtering methods since a FWT scheme does not offer advantage. This is because the expected frequency components of the current (at 10 Hz here) are known in advance. Hence, a filter can be specifically designed for that case.

3.2.2. *Using wavelets to extract uncertain frequency components*

The FWT scheme did not offer advantage in the simple filtering for denoising application described in the previous section. However, if the frequency information of the signal is time varying and its frequency is unknown the situation is different. Simple FIR filters cannot readily be used when there is useful information in the current signal in different and unknown areas of the frequency spectrum. Hence, the FWT comes into its own in such applications where the bandwidths are uncertain, or if useful components exist at widely spread frequencies. Applications in electrical drives which fit this profile include where signal injection schemes are used for sensor-less control for speed identification. This is an active research area [19–21]. In such a scheme a typical frequency spectrum may be as depicted in Fig. 10.

If the high frequency component is time varying but is remote in frequency from the useful low frequency components then low pass FIR filters are feasible. If the location of both coefficients was known then a filter bank with two FIR filters could be used, one low pass and one band pass. But this is not applicable here so this is a suitable application for wavelets. Unlike the application given in the previous section a fair comparison with a fixed FIR filter is difficult. Such a comparison could be made relatively favourable or unfavourable depending on the use of knowledge of the frequencies from a particular example, but this is not available online.

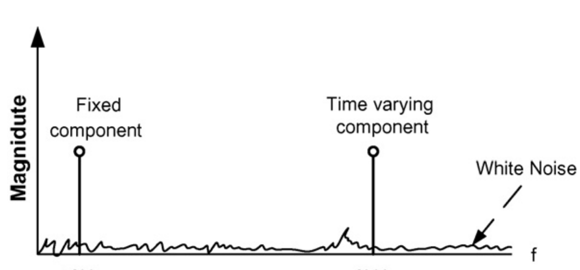

Fig. 10. Illustrative frequency spectrum with signal injection.

As an example of wavelet use in such a case, assume one component at 50 Hz resulting from the machine speed and another component ranging over [1.5 kHz, 2.5 kHz] (a test signal at 2 kHz is used), sampling frequency 100 kHz (this is required since the useful signal now is 200 times higher in frequency than before). To mimic a typical case a white noise signal is added giving a SNR of 10. This produced a random signal, with Gaussian distribution, zero mean value and a variance of 0.1.

The two useful frequency components come from two sine waves of amplitude 10. To evaluate the denoising process the mean squared error (MSE) of the original noise free and the two denoised signals is used:

$$\mathrm{MSE} = \frac{1}{N}\sum_{n=1}^{N}(x(n) - \tilde{x}(n))^2 \tag{10}$$

where $x(n)$ is the noised free signal and $\tilde{x}(n)$ is the signal under consideration.

The duration of the simulation was chosen to be 0.5 s giving 50,000 samples. The MSE of the noised and the noised free signal is ∼0.1.

Also for the FWT the principle of "superposition" holds, i.e. the values of CD1, CD2 and CA2 from the decomposition of two signals are the values given if the two signals are decomposed separately and then added together. Hence, the two sine waves (the useful signals) and the noise signals can be studied separately. The decomposition of the two sine waves gave three new signals whose histograms are shown in Fig. 11. Fig. 12 shows the histograms of the noise signal with the same scales.

Hence, if all the values of CD1, CD2 and CA2 that are between [−1, 1] are removed (hard thresholding) it can be assumed that all the noise components will be removed as well. These values of ±1 are empirically found, if Stein's Unbiased Risk method is used then the threshold is ±4.0332. Other, less conservative, techniques, such as Heuristic Stein's Unbiased Risk, produced similar thresholds. This gives a signal whose MSE with the original is 0.0277, i.e. five times better than the

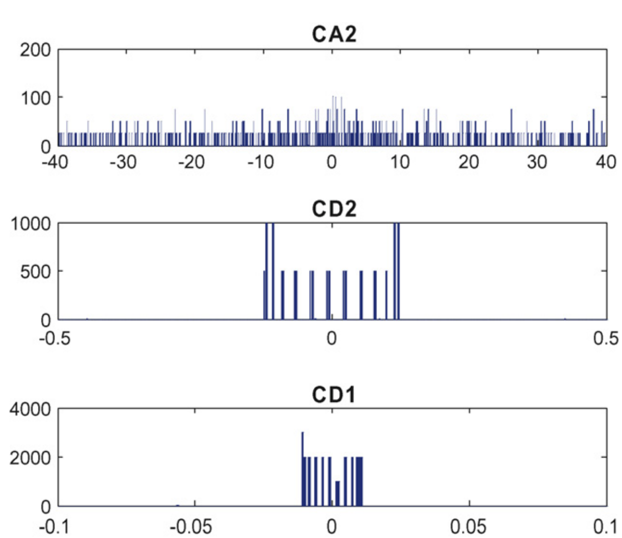

Fig. 11. Histograms of the approximations and details of the two sine waves.

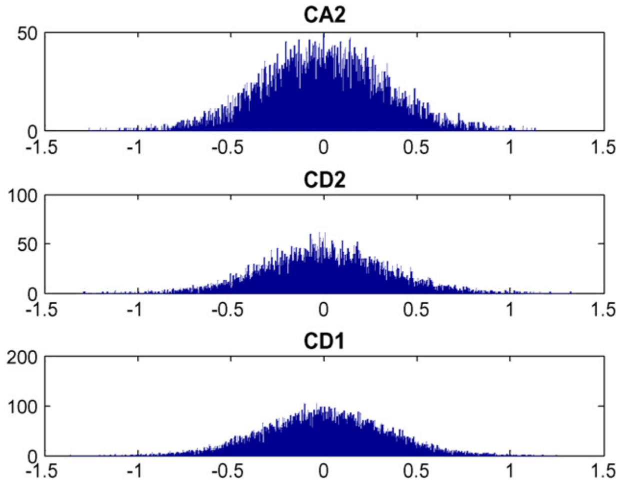

Fig. 12. Histograms of the approximations and details of the noise signal.

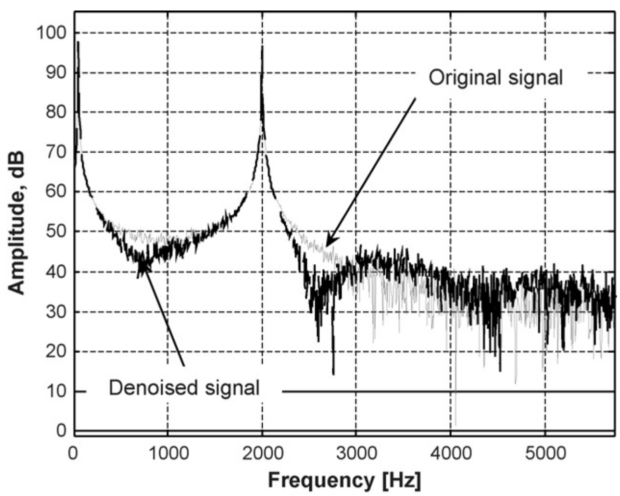

Fig. 13. Frequency spectrum of the original and denoised signals.

noisy signal. A comparison of the frequency spectra of the original and denoised signals is shown in Fig. 13, with an extended frequency range in Fig. 14 showing the improvement at the higher frequencies. The wavelet used was DB5.

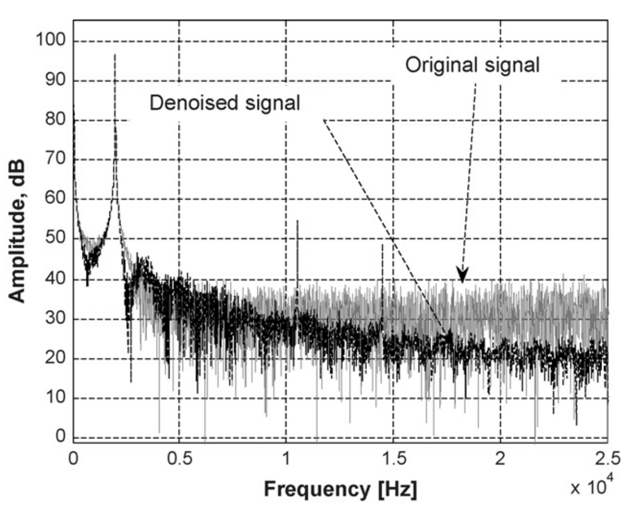

Fig. 14. Extended frequency spectrum of the original and denoised signals.

More levels or more advanced wavelet techniques (wavelet packets) can achieve better results. The important point is that this denoising did not require knowledge of its frequency components. It is simply assumed that the useful information has large coefficients and this illustrates the power of denoising based on the WT. Where the frequency components of the useful signals are unknown use of wavelets offers significant advantage since conventional method (such as fixed FIR filters) cannot easily used.

4. Conclusions

The WT was described, focusing on use for electric drives, and a denoising scheme based on it was proposed. The results were experimentally verified and it was found that the denoising scheme based on the WT did not distort the signal and the noise component after the process was small. However, the new scheme imposes a certain delay on the signal and is relatively complicated. The experimental results showed no obvious superiority for the new filtering scheme against more classical methods, in a relatively fixed frequency situation.

This indicates clearly that WT are best deployed in a more challenging situation, where useful components exist at widely spread and varying frequencies and the bandwidths are uncertain. Precisely this situation exists in electrical drive speed sensor-less control using signal injection. Results of a study have been presented, and confirm this view.

Acknowledgement

The authors wish to acknowledge the support of Control Techniques for this and related work.

References

[1] O. Rioul, M. Vetterli, Wavelets and signal processing, IEEE Sig. Proc. Mag. 8 (October (4)) (1991) 14–38.
[2] M. Vetterli, C. Herley, Wavelets and filter banks: theory and design, IEEE Trans. Sig. Proc. 40 (September (9)) (1992) 2207–2232.
[3] I. Daubenchies, The wavelet transform, time–frequency localisation and signal analysis, IEEE Trans. Inf. Th. 36 (September (5)) (1990) 961–1005.
[4] S.G. Mallat, A theory for multiresolution signal decomposition: the wavelet representation, IEEE Trans. Pat. Anal. Mach. Intel. 11 (July (7)) (1989) 674–693.
[5] S. Fedrigo, A. Gandelli, A. Monti, F. Ponci, A unified wavelet-based approach to electrical machine modelling, in: IEMDC, 2001, IEEE International, 2001, pp. 765–769.
[6] C.M. Arturi, P. Fedrigo, A. Gandelli, S. Leva, A.P. Morando, Dynamic analysis of electromechanical converters by means of the wavelet transform, in: Proceedings of the IEEE 1999 International Conference on Power, Electricity & Drive Systems, 1999, PEDS'99, vol. 1, July 27–29, 1999, pp. 462–466.
[7] C.L. Lin, N.C. Shieh, P.C. Tung, Robust wavelet neuro control for linear brushless motors, IEEE Trans. Aero Electr. Syst. 38 (July (3)) (2002) 918–932.
[8] S. Khorbotly, A. Khalil, J. Carletta, I. Husain, A wavelet based de-noising approach for real-time signal processing in switched reluctance motor drives, in: IECON 2005, November 6–10, 2005, pp. 1437–1442.
[9] B. Hubbard, in: A.K. Peters (Ed.), The World According to Wavelets, the Story of a Mathematical Technique in the Making, Wellesley, Massachusetts, 1995, ASIN: 1568810474.

[10] I. Daubenchies, Ten Lectures on Wavelets, Capital City Press, Montpelier, Vermont, 1992.
[11] Y. Meyer, Wavelets, Algorithms & Applications (translated and revised by R.D. Ryan), SIAM, Philadelphia, 1993.
[12] G. Strang, T. Nguyen, Wavelets and Filter Banks, Wellesley, Cambridge, 1996.
[13] H. Douglas, P. Pillay, A.K. Ziarani, A new algorithm for transient motor current signature analysis using wavelets, IEEE Trans. Ind. Apps. 40 (September/October (5)) (2004) 1361–1368.
[14] L. Eren, M.J. Devaney, Bearing damage detection via wavelet packet decomposition of the stator current, IEEE Trans. Instrum. Meas. 53 (April (2)) (2004) 431–436.
[15] B.A. Jont, R.R. Lawrence, A unified approach to short time Fourier analysis and synthesis, IEEE Proc. 65 (November (11)) (1977) 1558–1564.
[16] L.D. Donoho, De-noising by soft-thresholding, IEEE Trans. Inf. Th. 41 (May (3)) (1995) 613–627.
[17] S. Grace Chang, Y. Bin, M. Vetterli, Adaptive wavelet thresholding for image denoising and compression, IEEE Trans. Image Proc. 9 (September (9)) (2000) 1532–1546.
[18] D. Gnanadurai, V. Sadasivam, An efficient adaptive thresholding technique for wavelet based image denoising, Int. J. Sig. Proc. 2 (2) (2005) 114–119.
[19] F. Briz, M.W. Degner, A. Diez, R.D. Lorenz, Static and dynamic behavior of saturation-induced saliencies and their effect on carrier-signal-based sensorless AC drives, IEEE Trans. Ind. Apps. 38 (May/June (3)) (2002) 670–678.
[20] M. Linke, R. Kennel, J. Holtz, Sensorless position control of permanent magnet synchronous machines without limitation at zero speed, in: IECON 2002, vol. 1, November 5–6, 2002, pp. 674–679.
[21] J. Holtz, Sensorless control of induction machines—with or without signal injection? Overview paper, IEEE Trans. Ind. Elect. 53 (January (1)) (2006) 7–30.